

# Optical system of a micro-nano high-precision star sensor based on combined stray light suppression technology

YAO MENG,<sup>1</sup> XING ZHONG,<sup>1,2,3,\*</sup> YONG LIU,<sup>1</sup> KUN ZHANG,<sup>2</sup> AND CHI MA<sup>1</sup>

<sup>1</sup>Changguang Satellite Technology Co., Ltd., Changchun 130102, China

<sup>2</sup>Changchun Institute of Optics, Fine Mechanics and Physics, Chinese Academy of Sciences, Changchun 130033, China

<sup>3</sup>State Key Laboratory of Structural Analysis for Industrial Equipment, Dalian University of Technology, Dalian 116024, China

\*Corresponding author: ciomper@163.com

Received 28 September 2020; revised 10 December 2020; accepted 10 December 2020; posted 11 December 2020 (Doc. ID 411134); published 18 January 2021

The micro-nano design of a high-precision star sensor is studied. Point source transmittance (PST, the ratio of the irradiance generated by the external field source on the image surface to the irradiance at the entrance pupil) is used as the evaluation index of stray light suppression ability, the stray light suppression theory of star sensors is analyzed, and the mathematical model between stray light suppression ability and detectable magnitude is established. In view of the limited volume of micro-nano star sensors, a new design principle of combined anti-stray-light design of the baffle and optical system is proposed. The high stray light suppression of the micro-nano star sensor is realized by using the imaging optical path design of active stray light suppression and the design of a conical extinction cavity, which breaks through the technical problem of coupling system volume and stray light suppression ability. The results of the simulation and on-orbit experiments show that the star sensor based on the joint stray light technology can achieve a PST of  $2 \times 10^{-8}$  at the avoidance angle under the premise of limited optical system volume, and it has a stray light suppression ability of 6.5 magnitude stars. © 2021 Optical Society of America

<https://doi.org/10.1364/AO.411134>

## 1. INTRODUCTION

Star sensors are astronomical navigation devices based on star recognition. So far, the star sensor is the most sophisticated and minimally drifting space attitude measuring component, and it has been widely used in aerospace, guidance, and navigation applications [1]. Since the birth of the first star sensor in the 1970s, accuracy improvement has been the most important technical issue in this area. At present, the most accurate star sensor can reach subarcsec attitude accuracy, while the mainstream high-precision star sensor's accuracy is better than  $3''$  ( $3\sigma$ ). Due to the development of the satellite industry in recent years, the trend of spacecraft manufacturing has gradually been transformed from large satellite platforms led by national missions to small satellite networking modes led by commercial companies. Therefore, the research and development of micro-nano star sensors for small satellite platforms has become a major research direction. Meanwhile, due to diversified requirements of commercial satellite missions, the precision requirements of micro-nano star sensors have become increasingly stringent, and high-precision product categories need to be achieved. However, according to the design mechanism of the star sensor, there is a coupling relationship between system accuracy and

overall size, so it is difficult to achieve micro-nano design of a high-precision star sensor.

Based on the design principle of star sensors, the accuracy depends on the number of detected stars, so the detection sensitivity is an important performance indicator of the star sensor [2]. Key reasons of why it is difficult to accomplish micro-nano design for traditional high-precision star sensor are as follows. The actual working environment of the star sensor is often under the stray light coming from the Sun or the Earth, which causes strong background noise. Therefore, in order to detect high-magnitude stars, methods such as increasing the optical aperture or lengthening the lens hood are usually used. Although these methods can effectively improve the count of signal electrons, they will also lead to a significant increase in system size and design difficulty [3,4]. Therefore, the influence of stray light on the star detection sensitivity is analyzed, and a design method is adopted in which the hood and the optical system are jointly considered to eliminate the stray light, thereby greatly reducing the length of the external hood and the size of the whole device.

## 2. STRAY LIGHT SUPPRESSION THEORY OF STAR SENSORS

### A. Analysis of Stray Light Suppression Ability

In order to improve the accuracy of attitude control, spacecraft use two star sensors to achieve dual vector positioning, that is, the pitch and yaw axis with higher accuracy of the star sensor are used as the control axes of the spacecraft [5,6]. The expression of pitch/yaw accuracy is

$$\sigma_{c-b} = \frac{\text{Error}_{\text{single}}}{\sqrt{N_{\text{star}}}} = \frac{\text{FOV} \cdot \sigma_{\text{centroid}}}{N_{\text{pixel}} \sqrt{N_{\text{star}}}}, \quad (1)$$

where  $\text{Error}_{\text{single}}$  is the accuracy of a single star measurement, FOV is the field of view,  $N_{\text{pixel}}$  is the number of sensor pixels,  $\sigma_{\text{centroid}}$  is the subdivision precision of centroid interpolation, and  $N_{\text{star}}$  is the average number of stars detected within the field of view. According to Eq. (1), the pitch and yaw accuracy of the star sensor are mainly determined by  $\text{Error}_{\text{single}}$  and  $N_{\text{star}}$ . But the single star measurement accuracy is limited by the performance of detectors, so it can hardly achieve technological breakthroughs in the short term. The improvement of overall accuracy of star sensors is usually realized by increasing the number of identifiable stars.

The number of identified stars is determined by the FOV and the detection sensitivity. The number of identifiable stars is proportional to the FOV, but the increase of the FOV will reduce the accuracy of single-star measurement. Therefore, how to improve the detection sensitivity becomes a key technical issue for the star sensor. The detection sensitivity is determined by the optical system signal-to-noise ratio (SNR) [7], whose function expression is as shown in Eq. (2):

$$\text{SNR} = \frac{S}{\sqrt{S + B + \sum N_{\text{ele}}^2}} \geq V_{\text{th}}, \quad (2)$$

where  $S$  is the count of signal electrons,  $B$  is the number of background noise electrons,  $N_{\text{ele}}$  is the number of noise electrons of the detector, and  $V_{\text{th}}$  is the signal-to-noise ratio threshold. The number of signal electrons is determined by many factors such as the detection star magnitude, the aperture [8,9], and so on, and the relationship is expressed as

$$S = \frac{A_l \cdot \tau \cdot E_0 \cdot 2.512^{-M_v} \cdot t \cdot K_{\text{fill}} \cdot QE}{E_{\text{ph}} \cdot N^2}, \quad (3)$$

where  $A_l$  is the entrance area of the optical system,  $\tau$  is the transmittance of the optical system,  $E_0$  is the irradiance of the zero-magnitude star,  $M_v$  is the detection magnitude,  $t$  is the integration time,  $K_{\text{fill}}$  is the detector fill factor,  $QE$  is the detector quantum efficiency,  $E_{\text{ph}}$  is the energy of a single photon, and  $N$  is the diffusion factor.

Although the background noise is an indicator parameter during the design process, in order to reduce the design variables, the designer will not consider its change caused by stray light, but estimate the background noise as the radiation

intensity of a star of 10 magnitudes. However, under actual working conditions, the suppression of stray light is not ideal, and the residual stray light after being suppressed by the hood will enter the optical system and be scattered or even reflected to the focal plane. The stray light from outside the avoidance angle will greatly reduce the SNR of the star point image. The background noise  $B$  can be expressed [10] as

$$B = \frac{A_l \cdot \tau \cdot E_b \cdot t \cdot K_{\text{fill}} \cdot QE \cdot a^2}{f^2 \cdot E_{\text{ph}}}, \quad (4)$$

where  $E_b$  is the irradiance of the stray light at the detector,  $a$  is the pixel size, and  $f$  is the focal length of the system.

The star sensor belongs to the dark target detection system, and stray light is formed by light outside the imaging FOV. When the stray light illumination is higher than the threshold value of the detected star signal, the star SNR will not be able to meet the star point extraction requirements; therefore, the maximum allowed stray light irradiance avoidance angle (the angle is much larger than the FOV) must be taken as the benchmark to evaluate the stray light suppression capability of the system. In the optical index system, the point source transmittance (PST) is mainly used as the evaluation index to evaluate the suppression ability of out-of-field stray light. The physical meaning of PST is the ratio of the irradiance generated by the external field source on the image surface  $E_i(\theta)$  to the irradiance at the entrance pupil  $E_e(\theta)$ . That is, the ratio of the mixed illuminance after suppression to the illuminance at the entrance

$$\text{PST}_{\text{sys}} \leq \frac{E_i(\theta)}{E_e(\theta)}, \quad (5)$$

where  $E_i$  is the irradiance of stray light on the detector. According to Eqs. (2)–(5), the background irradiance of the limit star when the SNR threshold can be obtained, which is the maximum allowable stray irradiance at the image plane:

$$E_i = E_b = \frac{f^2 \cdot A_l \cdot \tau \cdot E_0^2 \cdot 2.512^{-2M_v} \cdot t \cdot K_{\text{fill}} \cdot QE}{V_{\text{th}}^2 \cdot E_{\text{ph}} \cdot N^4 \cdot a^2} - \frac{f^2 \cdot E_0 \cdot 2.512^{-M_v}}{N^2 \cdot a^2} - \frac{f^2 \cdot \sum N_{\text{ele}}^2 \cdot E_{\text{ph}}}{A_l \cdot \tau \cdot a^2 \cdot t \cdot K_{\text{fill}} \cdot QE}. \quad (6)$$

The high-energy stray light source in the space is mainly dominated by the Sun, while the response spectrum of the star sensor detector is mainly concentrated in the range of 500 to 900 nm. Therefore, the irradiance  $E_e$  of the solar stray light can be expressed as

$$E_e = \int_{0.5}^{0.9} \frac{2\pi h c^2}{\lambda^5} \frac{1}{e^{ch/(\lambda k T)} - 1} d\lambda, \quad (7)$$

where  $h$  is the Planck constant,  $T$  is the temperature,  $c$  is the light speed, and  $k$  is the Boltzmann constant. According to the relationship between the limit magnitude and the background value, the PST of the system can be expressed as

$$\text{PST}_{\text{sys}} \leq \frac{1}{\int_{0.5}^{0.9} \frac{2\pi h c^2}{\lambda^5} \frac{1}{e^{ch/(\lambda k T)} - 1} d\lambda} \left( \frac{f^2 \cdot A_l \cdot \tau \cdot E_0^2 \cdot 2.512^{-2M_v} \cdot t \cdot K_{\text{fill}} \cdot QE}{V_{\text{th}}^2 \cdot E_{\text{ph}} \cdot N^4 \cdot a^2} - \frac{f^2 \cdot E_0 \cdot 2.512^{-M_v}}{N^2 \cdot a^2} - \frac{f^2 \cdot \sum N_{\text{ele}}^2 \cdot E_{\text{ph}}}{A_l \cdot \tau \cdot a^2 \cdot t \cdot K_{\text{fill}} \cdot QE} \right). \quad (8)$$

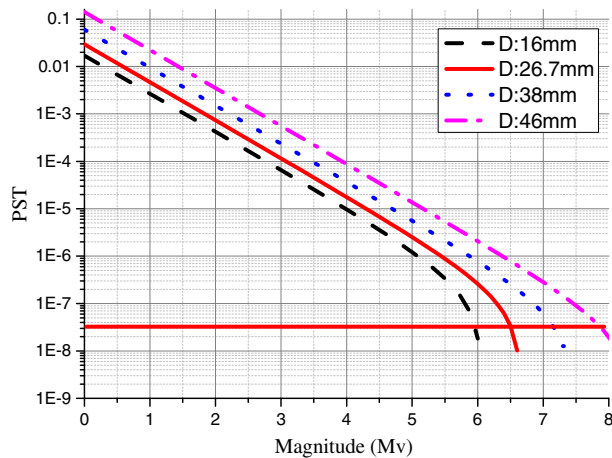


**Fig. 1.** PST curve under different apertures for different star magnitudes.

Equation (8) is analyzed by taking the parameters of a typical high-sensitivity star sensor as an example. The SNR threshold  $V_{th}$  is 5, the detected limit magnitude is 6.5 Mv, the focal length  $f$  is 40 mm, and the optical system transmittance  $\tau$  is 0.9. The integration time is 80 ms, the diffusion factor is 3, the detector pixel size is  $5.3 \mu\text{m}$ , and the quantum efficiency is 0.6 in the visible spectrum. Finally, the PST curve of the system under different apertures for different star magnitudes is shown in Fig. 1.

According to the figure, for a typical star sensor with an F-number of 1.5 (optical aperture: 26.7 mm), the PST of the system for solar avoidance should be at least better than  $2 \times 10^{-8}$ .

## B. Theoretical Study on Combined Stray Light Suppression

The stray light suppression of a star sensor is realized by an external hood. The design principle of a star sensor should follow the principle that the light in the FOV is not blocked, and the stray light line outside the avoidance angle should be scattered into the optical system many times. The stray light suppression ability of the hood is determined by its stages. The higher the number of stages, the more scattering times of stray light there will be, and the stronger the stray light elimination ability will be, but the volume will be larger. In the case of a traditional primary hood (single hood), the stray light is generally scattered within 3 times, and the stray light absorption rate of 1 time (the absorption rate of single stray light) is generally between 96% and 98%, that is, the  $PST_{baffle}$  of the hood should be within the range of  $10^{-5}$  to  $10^{-6}$ , and the critical scattering path of stray light is shown in Fig. 2.

In general, the hood is designed independently from the lens, that is, the lens is treated as a “black box” in the process of designing the hood, and the stray light scattering characteristics inside the lens are not considered. In fact, the transmission path of the residual scattered light suppressed by the hood in the lens is not fixed. The traditional design method is to put the optical system in the process of “passive” stray light elimination. The suppression of stray light by the lens will present nonlinear characteristics, and the peak  $PST_{lens}$  of the lens is lower than

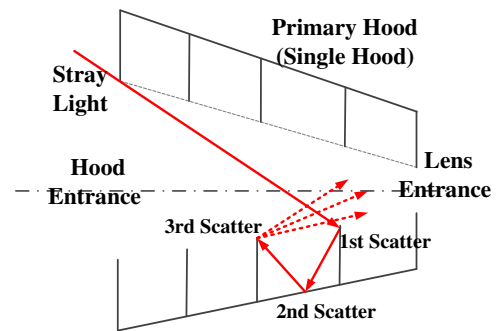


**Fig. 2.** Stray light critical scattering path of the primary hood.

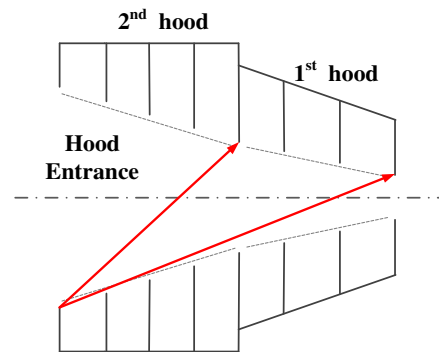


**Fig. 3.** Typical two-stage hood design.

the order of  $10^{-1}$ , which will lead to the stray light suppression ability of the system being no better than  $1 \times 10^{-7}$ . Therefore, the stray light suppression capability of the primary hood cannot meet the high-precision design requirement. In order to achieve the stray light suppression ability of a high-precision star sensor, a two-stage structure hood is usually used to improve the stray light suppression capability of the star sensor.

A typical two-stage hood design is shown in Fig. 3. The part close to the lens is the first-stage hood, which mainly suppresses light from the atmosphere, while the second-stage hood acts to suppress sunlight. At present, the hood design is mainly based on absorption, cooperating with a special-shaped light blocking ring or a sawtooth light blocking ring to achieve high a stray light suppression capability of the hood itself.

The function expression of the two-stage hood length [11,12] is

$$L = \frac{D(\tan \omega + \tan \beta)}{(\tan \beta - \tan \alpha)(\tan \alpha - \tan \omega)}, \quad (9)$$

where  $L$  is the length of the hood,  $\alpha$  and  $\beta$  are the stray light suppression angles,  $\omega$  is the field of view, and  $D$  is the optical aperture of the first piece of the lens.

Although the traditional two-stage hood can effectively suppress external stray light, according to Eq. (9), the volume of the two-stage hood is not only the superposition of two first-stage hoods but also with a certain degree of magnification. This will lead to an increase in the volume of the whole system. Therefore, it is necessary to improve the stray light suppression efficiency of the whole system link.

Different from the traditional design idea of the simple hood, the combined stray light suppression is to decompose

the coupling relationship between the hood and the lens and carry out collaborative design according to the relationship between them. The specific design idea is based on the scattering path of the residual stray light in the lens after the primary hood suppression, so as to achieve the “active” stray light suppression effect in the lens, and finally to achieve the stray light suppression ability of the two-stage hood by using the combined optimization of the primary hood and the lens. This design method not only ensures the high level of stray light but also greatly reduces the system volume. Although the design principle is similar to that of the two-stage hood, the combined stray light suppression ability is performed on the detector. Therefore, in addition to the hood, the lens should also be considered a crucial part in the stray light suppression progress. At this time, the stray light suppression evaluation function of the whole system  $PST_{sys}$  can be expressed as

$$PST_{sys} = PST_{baffle}(D, \theta, L, \tau) \cdot PST_{lens}(D, \eta). \quad (10)$$

In Eq. (10),  $PST_{baffle}(D, \theta, \omega, \tau)$  is the point source transmittance of the hood, which is a function of the aperture  $D$ , the stray light suppression angle  $\theta$ , the hood length  $L$ , and the absorption rate  $\tau$ ;  $PST_{lens}(D, \eta)$  is the point source transmittance of the lens itself, which mainly depends on the aperture  $D$  and the stray light suppression efficiency  $\eta$  inside the lens. The traditional hood enhances  $PST_{baffle}(D, \theta, \omega, \tau)$  as the optimization direction of stray light suppression, so it ignores the importance of improving  $PST_{lens}(D, \eta)$ . In this paper, the system is optimized from two aspects. The first is to realize the suppression of both external and internal stray light by means of joint design of the optical system and hood altogether. The second aspect is to improve the stray light suppression efficiency of the optical system itself. The specific design principle is shown in Fig. 4.

According to the figure, the star sensor uses an external hood to avoid sunlight, so the stray light entering the lens is the Earth atmosphere light and the sunlight that has been scattered more than 3 times. Meanwhile, in order to realize the ability of eliminating stray light with a high rejection ratio, a specific stray light suppression design should be conducted according to the transmission path of the scattered light inside the lens.

### 3. OPTICAL SYSTEM DESIGN STAR SENSOR COMBINED WITH STRAY LIGHT SUPPRESSION

Stray light in lens comes from the arrival of light outside the field of view on the detector; it can be divided into external and internal stray light according to different transmission paths.

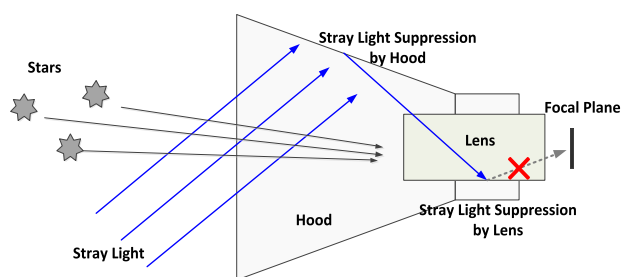


**Fig. 4.** Design principle of combined stray light suppression technology.

External stray light is direct radiation on the detector from the space environment, and it can be suppressed directly by an external hood, while the internal stray light comes from multiple scattering inside the lens barrel. It needs to analyze the parts that are sensitive to internal scattering and reflection and to optimize the internal structure and lens shape to cut off the stray light path to suppress the internal stray light.

#### A. Analysis of Stray Light Scattering Link

The internal stray light of a star sensor is mainly generated by multiple scattering during the suppression of external stray light by the hood. Scattering is an optical property that can happen on any medium surface, and its propagation direction is in the whole hemisphere. Therefore, it is impossible to block the transmission path of stray light via a single component. According to the design principle of the external hood, the stray light that is formed by the hood can enter the system after being scattered up to 3 times, and at this time, the lower wall of the retaining ring will become an external stray light scattering body. These surfaces can be approximately treated as a luminous body with a certain irradiation intensity and located outside the FOV. The retaining rings are as shown in Fig. 5. The light path in the figure is the path of the light after scattering 3 times on the retaining rings, which is also the path of stray light that is supposed to be suppressed.

As shown in Fig. 5, stray light scattered by the first-stage hood will directly enter the optical lens, and this light would arrive the focal plane if not properly suppressed. In this case, the background noise will reduce the sensitivity of the system and thus reduce the precision of the star sensor. The stray light joint elimination technology is specifically designed for this kind of scattering light, based on the analysis of stray light scattering paths and the geometric relationship between interior parts of the lens. Thus, the hood–lens joint design is carried out to reach the function of a two-stage hood, so as to realize the effect of high-intensity elimination of stray light.

#### B. Design of the External Hood Based on Active Control of the Scattering Link

Traditional star sensor design does not consider stray light suppression characteristics of the lens itself; the hood uses the first piece of the lens in the system as the avoidance surface. On the other hand, the joint stray light elimination technique treats the optical system as an “open” space of stray light suppression, which means that the whole space before the focal plane can

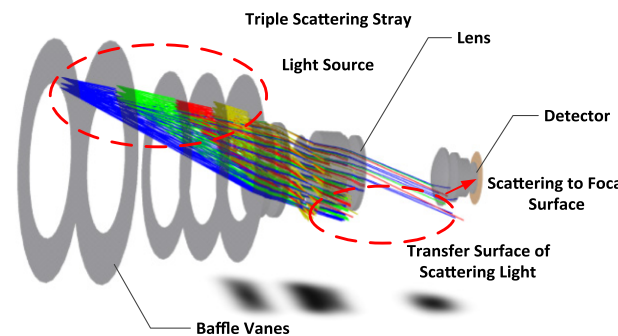


**Fig. 5.** Analysis of stray light transmission path.



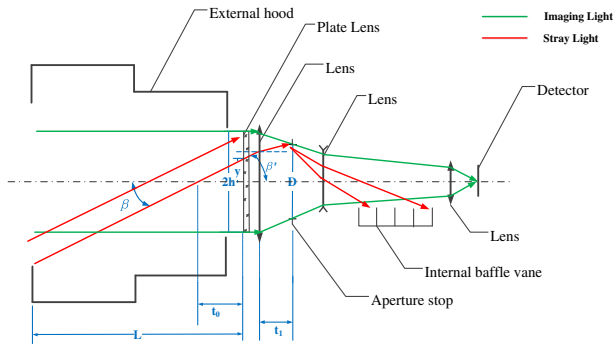


**Fig. 6.** Design principle of external hood for combined stray light suppression.

be used for stray light suppression. The main function of the aperture stop is to divide the imaging light and the nonimaging light, and therefore the aperture stop surface can be set as the stray light avoidance surface to reduce the hood length. The specific principle is shown in Fig. 6.

According to Fig. 6, using the aperture stop as the first set of retaining rings can suppress the stray light outside the  $\beta$  angle, and the length of the hood of this angle  $L_\beta$  can be calculated by a geometric relationship as follows:

$$L_\beta = \frac{t_0(h + y)}{y - t_0 \tan \omega}, \quad (11)$$

where  $h$  is the semi-diameter of the first lens,  $\omega$  is the half-field angle,  $y$  is the height of critical stray light projected onto the first group of lenses, and  $t_0$  is the distance from the intersection of the critical stray light and the lens's optical axis to the first group of lenses as shown in Fig. 5. When the optical system and the  $\beta$  angle are determined,  $y$  and  $t_0$  can be expressed as

$$y = \frac{D - 2t_1 \tan \beta}{2(1 - t_1 \phi)}, \quad (12)$$

$$t_0 = \frac{D - 2t_1 \tan \beta}{2 \tan \beta (1 - t_1 \phi)}, \quad (13)$$

where  $D$  is the aperture diameter,  $t_1$  is the interval between the aperture stop and the first lens group, and  $\Phi$  is the optical power of the first lens group. According to Eqs. (11)–(13), the length of the external hood can be calculated.

### C. Design of Conical Cavity Internal Stray Light Suppression

Based on the principle of combined stray light suppression, the scattered light in the lens is mainly formed by the three-time scattering by the hood, so it is necessary to suppress the scattering path in the lens according to the design of the hood. The traditional method of stray light suppression in the lens is mainly to set the extinction thread, while the optical system with strong demand for stray light suppression mainly uses the form of setting a light barrier in the lens to suppress stray light. However, for a star sensor system, there are lens elements and the lens seat and other components inside the lens, so space within the lens barrel is limited. It is impossible to use the simple geometric relationship during the hood design for derivation.

Therefore, it is necessary to optimize the stray light suppression structure in the lens based on the energy transfer theory of scattered light. According to the theory of radiation energy conduction, the expression of light energy propagating between two surfaces in the same medium is as follows:

$$d\phi_c = \frac{L_s(\phi_0, \varphi_0, \lambda_0) \cdot dA_s \cdot \cos \theta_s \cdot dA_c \cdot \cos \theta_c}{R^2}, \quad (14)$$

where  $d\phi_c$  is the light flux of the receiving surface;  $L_s(\phi_0, \varphi_0)$  is the illuminance of the light source surface;  $A_s$  and  $A_c$  are the area of the light source and the receiving surface;  $\theta_s$  and  $\theta_c$  are angles between the line connecting the light source surface center and the receiving surface center and their respective normals; and  $R$  is the length between the light source surface and the receiving surface. The first scattering of the light energy in the lens can be defined as the inter-surface propagating energy with different bidirectional reflection distribution function (BRDF) characteristics [13]. According to Eq. (14), the mathematical model of the first scattering light energy propagation with the detector as the receiving surface can be obtained as follows:

$$\phi_c = \pi \phi_s (\text{BRDF})(\text{GCF}), \quad (15)$$

where  $\phi_c$  is the power received by surface of the detector,  $\phi_s$  is the input light power onto the first scattering surface; BRDF is mainly used to describe the optical scattering characteristics of the structural surface of the optical machine, which is the ratio of the radiance  $L_s(\phi_0, \varphi_0, \lambda_0)$  in the output direction to the irradiance  $E_s(\phi_0, \varphi_0, \lambda_0)$  in the input direction; and GCF is the geometric parameter factor. According to Eq. (15), under the premise of a determined receiving surface, the stray light in the lens can be suppressed by the following two ways: (1) increasing the absorption capacity on the transmitting surface of the scattered light in the lens; (2) reducing the area of the transmitting surface. Based on the theory above, combined with the transmission path of the residual scattered stray light from the hood, a special-shaped extinction cavity is designed in the lens to achieve the best efficiency of stray light suppression.

Because the vector direction of the three-time scattered light by the baffle ring has strong directionality, it is suitable for directional suppression, and accordingly the system adopts a conical cavity structure [14,15]. The cavity is designed based on the envelope of the scattering light path. Baffle rings with different dip angles are designed to minimize the radiation area in the process of scattered light transmission. The spacings between the baffle rings are determined by the depth of the cavity. The “local absorption light traps” on the inner wall of the lens tube are realized by combining different dip angle settings. The specific design principle is shown in Fig. 7.

In Fig. 7, the baseline of the shield cylinder wall is taken as the symmetry axis, and the envelope line of the imaging light path works as an auxiliary line after being mirrored. Thus, after scattering by the inner wall of the shield, the edge stray light will travel into the inclined baffle ring so that the stray light can achieve more than 3 times scattering. In the figure,  $\alpha_i$  is the inclination angle of two adjacent baffle rings, which is the angle between the optical axis and the edge scattered light inside the lens,  $D$  is the exit pupil diameter of the extinction cavity,  $H$  is the diameter of the extinction cavity component,  $\omega$  is the FOV of the imaging optical path,  $L$  is the cavity length, and  $l_i$  is the

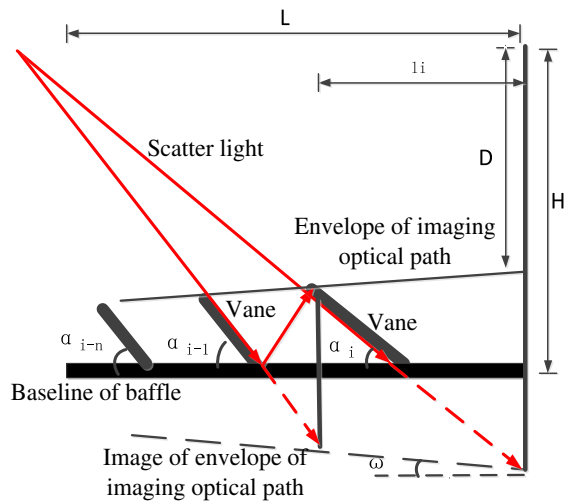


Fig. 7. Design principle of conical extinction cavity.

Table 1. System Indicators

| Parameter                      | Value      |
|--------------------------------|------------|
| Focal length                   | 40 mm      |
| $F$ number                     | 1.5        |
| Full field of view             | $10^\circ$ |
| Avoidance angle of stray light | $35^\circ$ |
| Detect magnitude               | 6.5 Mv     |

interval between the  $i$ th stage baffle ring and the exit end face of the extinction cavity. The angle between the special-shaped baffle ring and the light scattered onto it by the hood wall should be greater than  $90^\circ$  in order to ensure the stray light suppression efficiency. Therefore, on the condition that the length of the extinction cavity  $L$  is determined, the minimum extinction cavity diameter is as shown in Eq. (16):

$$\begin{cases} l_i = \frac{H-D}{\tan \alpha_i + \tan \omega} \\ l_{i-1} = \frac{2l_i \cdot \tan \alpha_i - H + D}{2(\tan \omega - \tan \alpha_i)} \\ \sum_{N=0}^n l_{i-N} = L \\ \alpha_{i-n} + \alpha_{i-n+1} \leq 90^\circ \end{cases}, \quad (16)$$

where  $\alpha_i$ ,  $\omega$ ,  $D$ , and  $L$  are all obtained from the design results of the optical system.  $l_{i-1}$  is the interval between the  $(i-1)$ th ring and the  $i$ th ring, and  $n$  is the number of rings. According to the equations, all parameters of the conical extinction module can be obtained.

#### 4. DESIGN EXAMPLE AND PERFORMANCE TEST OF THE OPTICAL SYSTEM BASED ON COMBINED STRAY LIGHT SUPPRESSION

##### A. Optical System Design Example

###### 1. System Indicators

Based on the design principle of joint stray light suppression, a high-precision micro-nano star sensor optical system with typical parameters is designed for the “Jilin-1” satellite platform. The system parameters are shown in Table 1.

###### 2. Design Method

In order to realize the overall design of the extinction cavity inside the lens, the optical system needs to adopt a large interval optical structure between the lens groups; based on the miniature design idea, the aperture stop of the system should be close to the front lens group. Meanwhile, the system demands high performance in field curvature correction, distortion correction, and energy concentration, together with a relatively large aperture, so a Cooke triplet lens is chosen as the initial structure of the system.

A Cooke triplet lens consists of two positive crown glass lenses on the outside and negative flint glass lenses in the middle. This kind of system has a large interval between the lens groups and strong independence and derivation. At the same time, this form also has the characteristics of low Petzval field curvature and low color difference, which thus will help to ensure the energy concentration on the detector plane, while the symmetry of the structure contributes to the adjustment of vertical aberrations such as distortion and coma. However, the residual aberration of the triplet lens is large, which is mainly high-order aberration such as spherical aberration and high-order astigmatism, and it will lead to a smaller relative aperture of the optical system and lower energy concentration of the star point. Because the spherical aberration is a high-order odd function of the system aperture, which is the main cause of the small relative aperture, it is necessary to correct the spherical aberration. Based on the functional relationship between spherical aberration and aperture, the crown-glass lens is split to reduce the aperture of the incident light to the lens, and thus the advanced spherical aberration of the system can be greatly reduced. At the same time, the high-order astigmatism and spherochromatic aberration in the system are reduced by increasing the optimization variables, and finally a negative lens is added near the focal plane to balance the residual field curvature of the system.

The condition of joint anti-stray light in Sections 3.B and 3.C is used as the boundary condition in optical design. The final optical design result is shown in Fig. 8(a), the system layout is shown in Fig. 8(b), and the sample product and installation status are shown in Figs. 8(c) and 8(d). In order to verify the performance of the product, the star sensor of the joint stray light elimination optical system was carried out on “Jilin-1 video 04 satellite,” which was successfully launched with the CZ-6 in the Taiyuan Satellite Launch Center at 12:50 Beijing time on 21 November 2017. So far, it works in normality in orbit.

###### 3. Analysis of the Stray Light Suppression Capability

In order to verify the stray light suppression ability of the star sensor, stray light tracings are carried out for systems of various design forms, with all the tracing results fitted into PST curves. The simulation results are shown in Fig. 9.

According to the simulation results, it can be seen that the system with a traditional primary hood cannot meet the detection requirements of high stars at  $35^\circ$  evasion angle; the optical system with the joint anti-stray light of the nonoptimized design has a rapid decline of PST at  $28^\circ$ – $30^\circ$ , that is, the system has entered the stray light suppression range, and the PST has a slow decline trend in the range of  $30^\circ$ – $35^\circ$ , which is composed of the aperture light of the lens. The PST outside  $35^\circ$  fluctuates

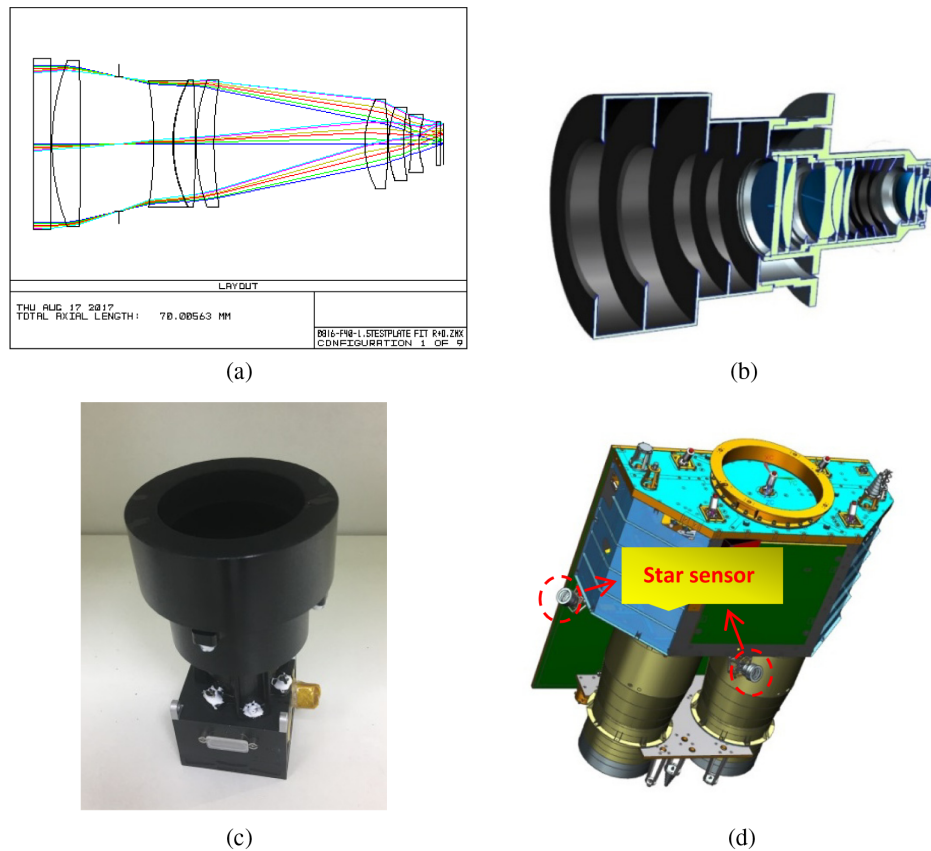


**Fig. 8.** Star sensor of combined stray light suppression. (a) Optical design result. (b) Optical system layout. (c) Sample product. (d) Installation status.

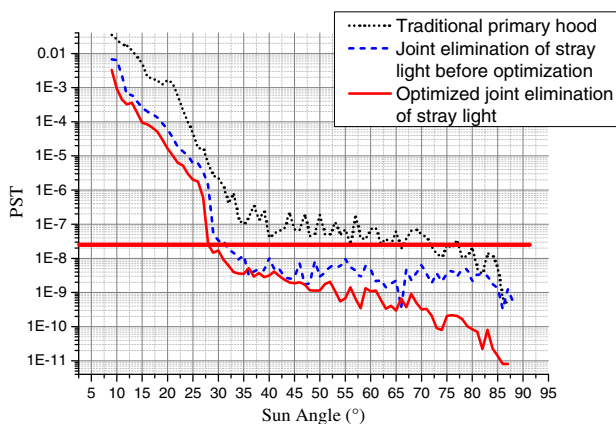


**Fig. 9.** PST curves figure.

steadily, which is the stage in which the external shield suppresses the solar stray light. After optimization, the system's ability to suppress stray light is better than before. At the same time, the decreasing rate of PST in the range of  $30^{\circ}$ – $35^{\circ}$  is obviously strengthened. It shows that the cone-shaped cavity hood has an obvious restraining effect on the internal scattered light of the optical system in front of the aperture, while the PST outside the restraining angle fluctuates slowly and decreases, which conforms to the design idea that the scattering surface of the cavity wall decreases with the increase of the incident angle.

## B. Verification on Orbit

In order to verify the stray light suppression ability of the combined stray light elimination system, the star sensor was tested for stray light on orbit. The specific test method is as follows: Adopting the inertial space imaging mode, the star-sensitive optical axis is used as the whole star direction, and the rotation direction is far away from the Sun incident direction until the star sensor fails. In order to ensure the independence of the stray light suppression angle test, the optical axis of the star sensor should avoid the influence of Earth light, that is, the angle between the star-sensitive optical axis and the satellite–Earth center connection is greater than  $120^{\circ}$ . The schematic diagram of the experiment is shown in Fig. 10.

The star sensor was tested on the Jilin01-sp04 platform, and the specific verification process and results are as follows: The satellite makes the optical axis vector of the star sensor under test and the Sun vector greater than  $60^{\circ}$  through the attitude adjustment. Telemetry was started at 04:01:30 on 14 January 14 2018, when the angle between the star-sensitive optical axis vector and the Sun vector was  $60.37^{\circ}$ .

Through maneuver adjustment, the attitude of the satellite was stabilized at 04:01:48 on 14 January 14 2018, and the on-orbit test was started. In the initial state, the angle between the star-sensitive optical axis vector and the Sun vector was  $56.19^{\circ}$ , and the whole star rotated at a speed of  $0.1^{\circ}/s$ , so the angle between the star-sensitive optical axis vector and the Sun vector decreased from large to small until the satellite lost its attitude

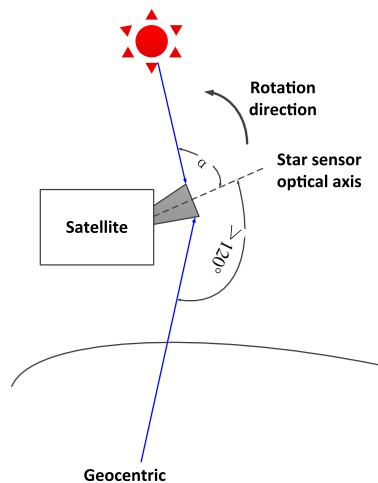


**Fig. 10.** Schematic diagram of stray light test on orbit.

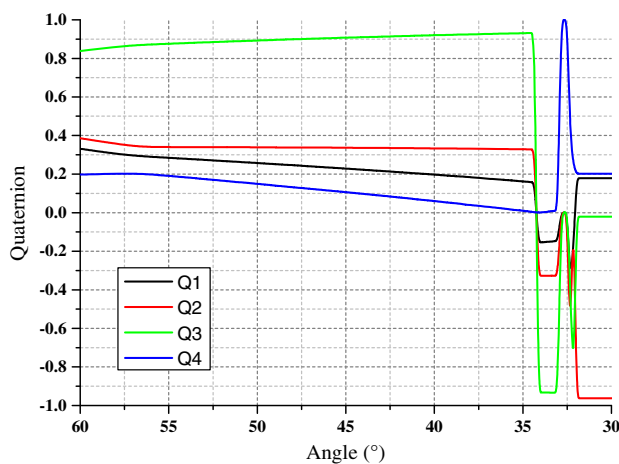


**Fig. 11.** Results of stray light test on orbit.

at 04:06:42 on 14 January 2018. At this time, the star-sensitive optical axis vector and the included angle of the Sun vector is  $34.58^\circ$ . The quaternion output of the star sensor in this test is shown in Fig. 11. It can be seen that when the evasion angle is less than  $34.58^\circ$ , the attitude quaternion jumps, and the final attitude is lost. That is to say, the stray light suppression angle of the joint stray light elimination optical system can meet the application requirements.

## 5. CONCLUSION

In this paper, the stray light transmission path between the hood and the optical system is theoretically tracked, and accordingly

the stray light suppression is realized with the optimizations on both the optical system and the hood. The numerical simulations reveal that even in a limited volume, the star sensor with stray light suppression function could still reach the PST value of  $2 \times 10^{-8}$  at the avoidance angle, and thus it can be adopted to detect 6.5 Mv stars. Besides numerical simulations, on-orbit verification was also implemented, which definitely proves that the proposed stray light suppression design can satisfy the requirements of the star sensor.

**Disclosures.** The authors declare no conflicts of interest.

## REFERENCES

1. G. Wang, F. Xing, M. S. Wei, T. Sun, and Z. You, "Optimization method for star tracker orientation in the sun-pointing mode," *Chin. Opt. Lett.* **15**, 081201 (2017).
2. J. Li, J. Liu, and G. Li, "Study on detection sensitivity of APS star tracker," *Proc. SPIE* **6723**, 67235F (2008).
3. K. Hiroyuki and S. Yukio, "New light shielding technique for shortening the baffle length of a starsensor," *Proc. SPIE* **4767**, 62–69 (2002).
4. F. W. Scgenkel, "A self-deployable high attenuation light shade spaceborne astronomical sensor," *Proc. SPIE* **0028**, 109–113 (1972).
5. Y. Dong, F. Xing, and Z. You, "Determination of the optical system parameters for a CMOS APS based star sensor," *J. Astronaut.* **25**, 663–668 (2004).
6. T. Sun, F. Xing, and Z. You, "Optical system error analysis of high accuracy star trackers," *Acta Opt. Sin.* **33**, 0323003 (2013).
7. Radio Company(USA), *Electrooptics Manual* (National Defence Industry, 1978) (in Chinese).
8. X. Zhong, J. Q. Jia, and G. Jin, "Detecting performance and overall design of airborne daytime star sensor for navigation," *Opt. Precis. Eng.* **19**, 2900–2906 (2011).
9. Y. Pan, H. Wang, N. Jing, Y. Shen, Y. K. Xue, and J. Liu, "Parameter selection and optical design of all-day star sensor," *Acta Opt. Sin.* **44**, 0122002 (2016).
10. S. Yang, T. Meng, and T. Y. Ma, "The optimum design of micro star tracker camera lens parameter," *Aerospace Control* **33**, 67–71 (2015).
11. J. P. Arnoux, "Star sensor baffle optimization: some helpful practical design rules," *Proc. SPIE* **2864**, 333–338 (1996).
12. R. P. Breault, Control of stray light, in *Handbook of Optics* (Mc Graw-Hill, 1995), Vol. **11**, Chapter 38, pp. 1–34.
13. W. Lucht, C. B. Schaaf, and A. H. Strahler, "An algorithm for the retrieval of albedo from space using semiempirical BRDF models," *IEEE Trans. Geosci. Remote Sens.* **38**, 977–998 (2000).
14. W. Lu, "The baffle design and result simulation of star sensor," *Opto-Electron. Eng.* **28**, 12 (2001).
15. R. P. Breault, "Vane structure design trade-off and performance analysis," *Proc. SPIE* **0967**, 92–96 (1988).